

## Research Article

# A Numerical Study on Gas Flow through Anisotropic Sierpinski Carpet with Slippage Effect

Shuxia Qiu,<sup>1,2</sup> Lipei Zhang,<sup>2</sup> Zhenhua Tian,<sup>3</sup> Zhouting Jiang,<sup>2</sup> Mo Yang <sup>1</sup> and Peng Xu <sup>2,4</sup>

<sup>1</sup>School of Energy and Power Engineering, University of Shanghai for Science and Technology, Shanghai 200093, China

<sup>2</sup>College of Science, China Jiliang University, Hangzhou 310018, China

<sup>3</sup>Institute of Geophysics and Geomatics, China University of Geosciences, Wuhan 430074, China

<sup>4</sup>State Key Laboratory Cultivation Base for Gas Geology and Gas Control, Henan Polytechnic University, Jiaozuo 454000, China

Correspondence should be addressed to Mo Yang; yangm@usst.edu.cn and Peng Xu; xupeng@cjlu.edu.cn

Received 13 February 2020; Revised 10 May 2020; Accepted 12 May 2020; Published 8 July 2020

Academic Editor: Wei Wei

Copyright © 2020 Shuxia Qiu et al. This is an open access article distributed under the Creative Commons Attribution License, which permits unrestricted use, distribution, and reproduction in any medium, provided the original work is properly cited.

A pore-scale model has been developed to study the gas flow through multiscale porous media based on a two-dimensional self-similar Sierpinski carpet. The permeability tensor with slippage effect is proposed, and the effects of complex configurations on gas permeability have been discussed. The present fractal model has been validated by comparison with theoretical models and available experimental data. The numerical results show that the flow field and permeability of the anisotropic Sierpinski model are different from that of the isotropic model, and the anisotropy of porous media can enhance gas permeability. The gas permeability of porous media increases with the increment of porosity, while it decreases with increased pore fractal dimension under fixed porosity. Furthermore, the gas slippage effect strengthens as the pore fractal dimension decreases. However, the relationship between the gas slippage effect and porosity is a nonmonotonic decreasing function because reduced pore size and enhanced flow resistance may be simultaneously involved with decreasing porosity. The proposed pore-scale fractal model can present insights on characterizing complex and multiscale structures of porous media and understanding gas flow mechanisms. The numerical results may provide useful guidelines for the applications of porous materials in oil and gas engineering, hydraulic engineering, chemical engineering, thermal power engineering, food engineering, etc.

## 1. Introduction

Fluid flow through natural and artificial porous media such as soils, rocks, minerals, sludge, ceramics, textile, food, paper, plants, tissues, organs, and fuel cell plays an important role in daily life and practical applications [1–3]. The permeability which represents the capability of a porous medium to permit the flow of fluids through its pore spaces is commonly used to characterize fluid flow through a porous medium. In order to determine the permeability, direct experimental measurement can be performed on a porous medium based on Darcy's law proposed in 1856 [4–7]. Although the measured permeability is accurate and reliable, it can only be applied to a particular kind of porous material. With the rapid development of computer technology, numerical simulation has become an effective method to estimate the permeability of porous media [8–13]. A few continuous models

including finite difference method (FDM), finite element method (FEM), finite volume method (FVM), and Monte Carlo method as well as lattice Boltzmann method (LBM) have been proposed to investigate fluid flow properties in porous media.

As one of the key macroscopic transport properties of a porous medium, the value of permeability depends on the microscopic structures of the medium. Therefore, pore-scale mathematical models on fluid flow through porous media are significant for predicting the permeability and understanding the physical mechanisms of fluid flow through porous media [14]. However, it is difficult to characterize the complex and irregular structures of porous media with traditional Euclidean geometry. Many porous materials are widely accepted to indicate fractal scaling laws, and fractal dimensions such as pore/mass fractal dimension, tortuosity and surface fractal dimensions, Hausdorff dimension, and

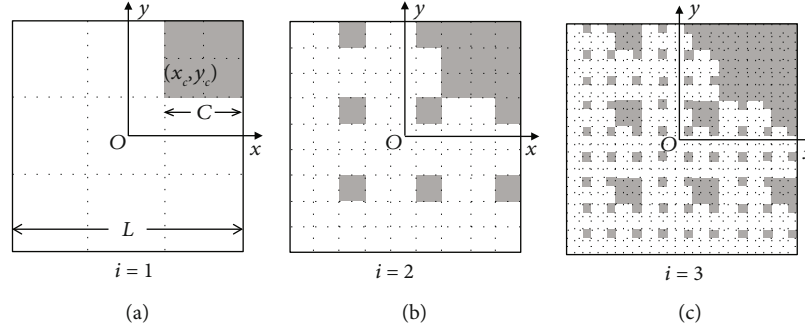


FIGURE 1: A schema for the construction process of the 2D Sierpinski carpet with  $s = 3$ ,  $n = 1$ ,  $\varepsilon_x = 1$ , and  $\varepsilon_y = 1$ : (a)  $i = 1$ , (b)  $i = 2$ , and (c)  $i = 3$  (white and gray areas represent solid and pore phases, respectively).

TABLE 1: Parameters of the isotropic Sierpinski carpet models.

Group no.	$s$	$n$	$D_f$	$\phi$				
				$i = 1$	$i = 2$	$i = 3$	$i = 4$	$i = 5$
S1	3	1	1.893	0.889	0.790	0.702	0.624	0.555
S2	4	4	1.792	0.750	0.563	0.422	0.316	0.237
S3	5	1	1.975	0.960	0.922	0.885	0.849	0.815
S4	5	9	1.723	0.640	0.410	0.262	0.168	0.107
S5	6	4	1.934	0.889	0.790	0.702	0.624	0.555
S6	6	16	1.672	0.556	0.309	0.171	0.095	0.053
S7	7	1	1.989	0.980	0.960	0.940	0.921	0.902
S8	7	9	1.896	0.816	0.666	0.544	0.444	0.363
S9	7	25	1.633	0.490	0.240	0.118	0.058	0.028
S10	8	4	1.969	0.938	0.879	0.824	0.772	0.724
S11	8	16	1.862	0.750	0.563	0.422	0.316	0.237
S12	8	36	1.602	0.438	0.191	0.084	0.037	0.016

spectral dimension have been proposed to characterize the fractal features governing the transport properties [15–21]. For example, Yu and Cheng [22] introduced pore and tortuosity fractal dimensions to characterize the pore structures and presented a fractal capillary bundle model for a single-phase flow through bidispersed porous media. Xu and Wei et al. [23, 24] presented analytical expressions for Kozeny-Carman constant by employing the pore fractal theory. While, Yu et al. and Xu et al. [25, 26] proposed analytical expressions for the relative permeability for the wetting and nonwetting phases with the assumption that pore size distribution follows statistically fractal scaling laws. Xu et al. [27] used fractal scaling laws to characterize the size and topology of the fracture system and presented a fractal network model for fluid flow through fractured porous media. Recently, Cai et al. [28] proposed a three-dimensional fractal model to characterize heterogeneous pore sizes in a shale stratum and presented an apparent permeability for shale. Except for fractal dimensions, Xia et al. [29] proposed two more fractal parameters (lacunarity and succolarity) to characterize the complex and irregular structures of porous media. Among various fractal models, the exactly self-similar Sierpinski carpet model with the flow path of simulating a wide range of pore sizes and configurations has long been used as a model substrate for solving transport problems through

TABLE 2: Parameters of the anisotropic Sierpinski carpet models.

Group no.	$s$	$n$	$D_f$	$\varepsilon_x$	$\varepsilon_y$
				A1	3
A2	4	4	1.792	1	0
A3	5	1	1.975	1	1
A4	5	9	1.723	1	0
A5	6	4	1.934	1	1
A6	6	16	1.672	1	0

natural porous media [30]. This fractal geometry is commonly adopted to model the complex pore space geometries of porous media, and different computational methods can be performed to develop pore-scale mathematical models for fluid flow through porous media [30–33]. However, most of fractal models are limited to isotropic porous media.

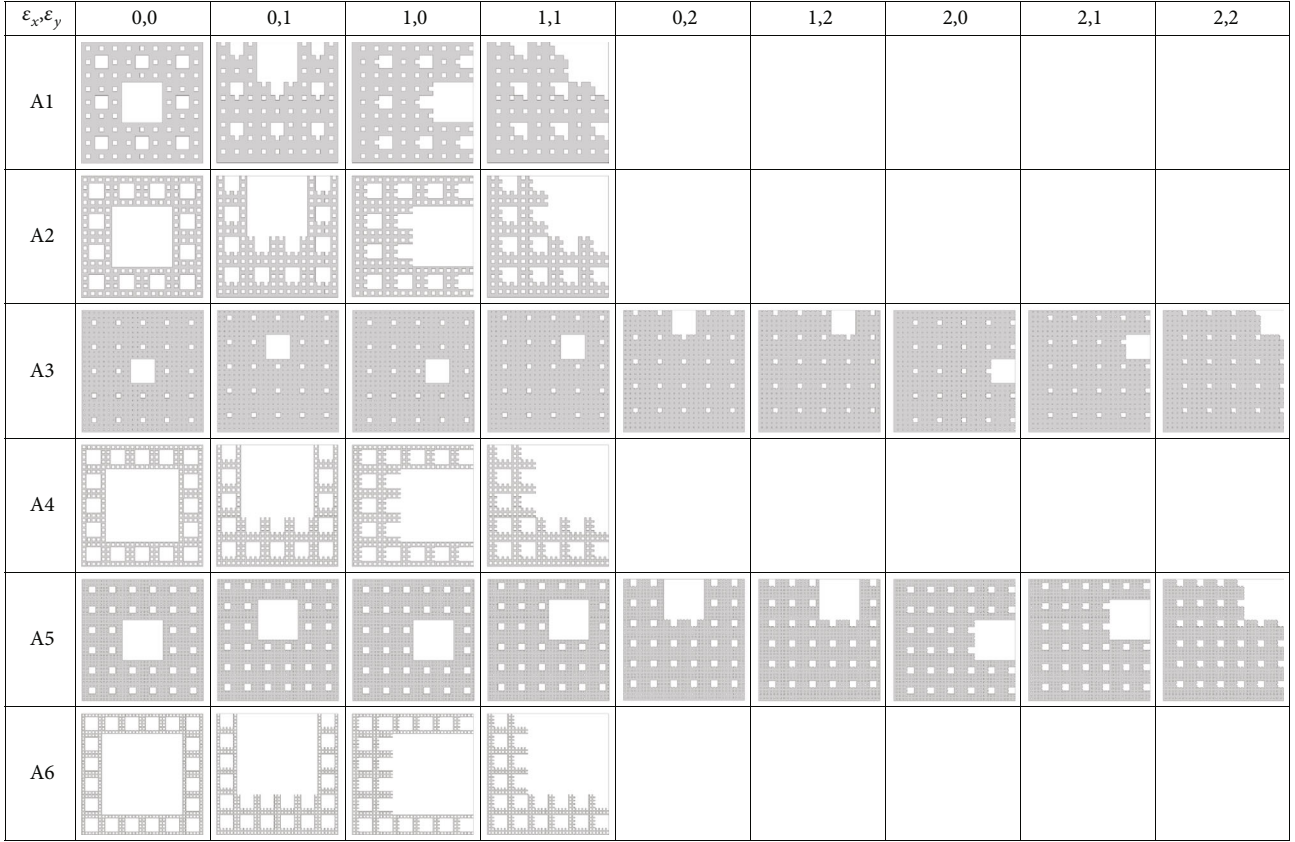


FIGURE 2: The 3rd order of the isotropic and anisotropic Sierpinski carpet models.

Because of the wide range of applications of anisotropic porous materials such as fibrous media, layered media, and rod bundles [34, 35], the discussions on fluid flow through anisotropic porous media are needed.

Recently, gas flow through microscale and nanoscale porous media has attracted increasing interests from science and engineering as it is of great significance for fuel cell, open-cell foams, membrane, microelectromechanical system, low-permeability reservoirs, energy storage devices, etc. [36–43]. When the gas molecule's mean free path is comparable to the pore size, the gas molecules and their collision with solid wall in the microscale and nanoscale pores takes an important effect on the gas flow [44, 45]. According to Klippenberg's effect, the rarefied gas effect should be taken into account for the fluid regime that the Knudsen number is greater than  $10^{-3}$ . However, the influence mechanisms of slippage effect on the permeability of anisotropic porous media are not clear. Therefore, the present work is aimed at developing a pore-scale model for gas flow through multiscale anisotropic porous media with slippage effect based on the Sierpinski carpet model and exploring the relationship between the macroscopic gas permeability and microscopic structures of porous media.

## 2. Fractal Model

In order to characterize the multiscale structures, an exactly self-similar Sierpinski carpet model is used to generate the

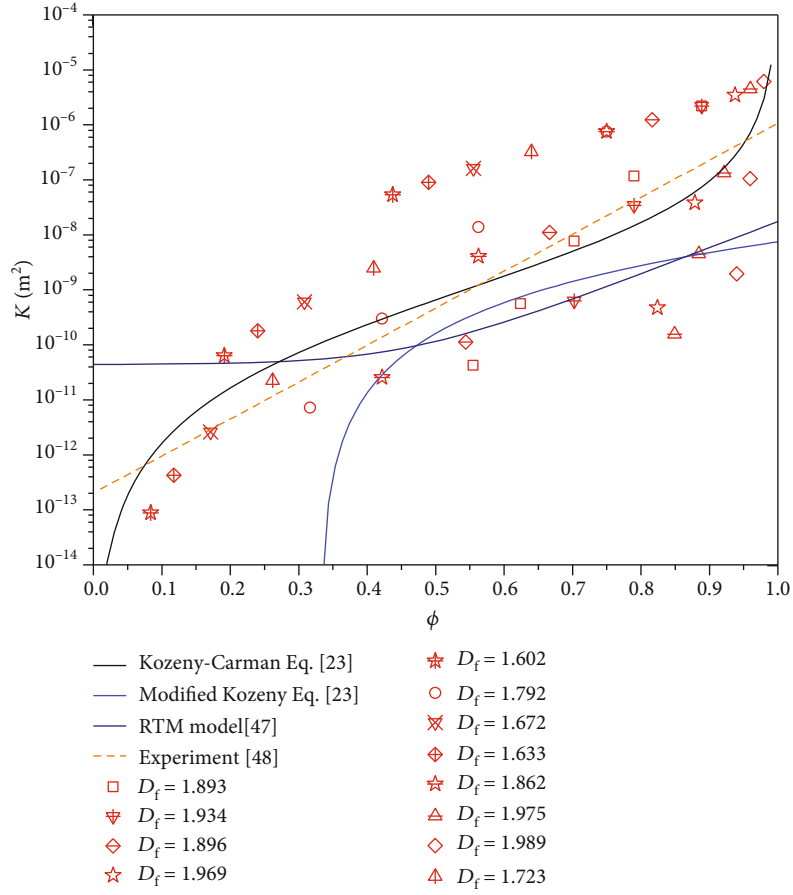
geometrical structure of the porous media. The 2D Sierpinski carpet model can be constructed by applying recursive algorithms on a void square with a size of  $L$ . Then,  $n$  square solid particles with size of  $C$  located at coordinate  $(x_c, y_c)$  are removed. The same procedure is recursively applied to the remaining squares in the next generation. Thus, the pore phase (gray area in Figure 1) in the present Sierpinski carpet model is exactly self-similar fractal, while the solid phase (white area in Figure 1) is nonfractal. That is, the statistical property of the pore size distribution of porous media can be characterized by the 2D Sierpinski carpet model. The pore fractal dimension can be calculated by [15, 46]:

$$D_f = \frac{\log(s^{D_E} - n)}{\log(s)}, \quad (1)$$

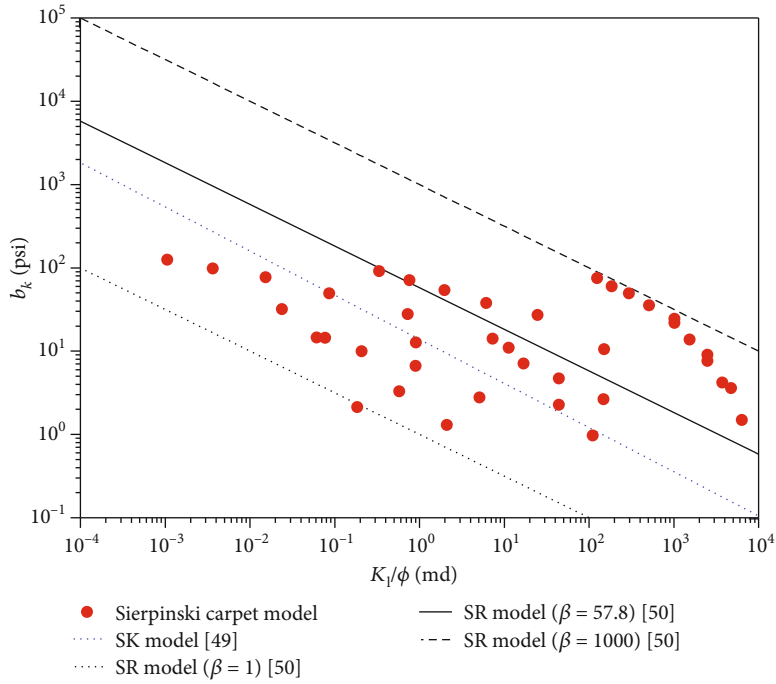
where the scaling factor is defined as  $s \equiv L/C$ , and the Euclidean dimension  $D_E = 2$  in a two-dimensional space. The area porosity of the  $i^{\text{th}}$  generation of the Sierpinski carpet model can be determined by

$$\phi_i = \left( \frac{s^{D_E} - n}{s^{D_E}} \right)^i. \quad (2)$$

The relationship between porosity and pore fractal dimension can be gotten by combining Equations (1) and (2).



(a)



(b)

FIGURE 3: A comparison of present numerical results with theoretical models and experimental data: (a) permeability without slippage effect and (b) gas slippage factor vs. absolute permeability.

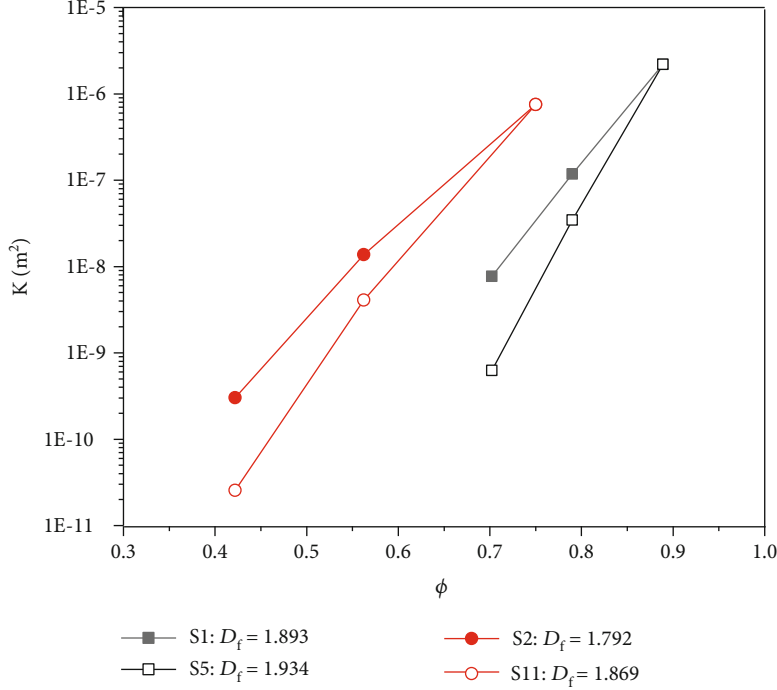


FIGURE 4: The effect of pore fractal dimension on the permeability of isotropic porous media.

$$\phi_i = (s^i)^{D_f - D_E} \tag{3}$$

In order to quantitatively characterize the anisotropic properties of porous media, two anisotropic factors are introduced.

$$\begin{aligned} \epsilon_x &= \frac{x_c}{C}, \\ \epsilon_y &= \frac{x_y}{C}. \end{aligned} \tag{4}$$

As shown in Figure 1, the anisotropic factors of  $\epsilon_x = 0$  and  $\epsilon_y = 0$  represent an isotropic Sierpinski carpet model, while the cases with  $\epsilon_x \neq 0$  or  $\epsilon_y \neq 0$  denote anisotropic Sierpinski carpet models. Table 1 lists the calculated pore fractal dimension and porosity of isotropic Sierpinski carpet models. The range of pore fractal dimension varies from 1.602 to 1.989, and the porosity value is in the range of 0.016 and 0.960. Due to computer capacity limitations, only five orders of the Sierpinski carpet model were simulated. The parameters of the anisotropic samples are summarized in Table 2. In order to compare the gas flow through anisotropic porous media with that of isotropic porous media, six groups of anisotropic Sierpinski carpet models (A1-A6) with the same pore fractal dimension and porosity as the isotropic Sierpinski carpet models (S1-S6) were used. Figure 2 shows an example of the 3rd order of the isotropic and anisotropic Sierpinski carpet models.

For the gas flow through porous media at very low Reynolds numbers, the inertial term in the Navier-Stokes equa-

tions can be neglected. Thus, the governing equations for a steady peristaltic flow of the incompressible Newtonian fluid through the Sierpinski carpet models are the continuity equation for the conservation of mass and Stokes equations for the conservation of momentum.

$$\rho \nabla \cdot \mathbf{u} = 0 \tag{5}$$

$$\nabla \cdot (P\mathbf{I} + \mathbf{H}) + \mathbf{F} = 0 \tag{6}$$

where  $\rho$  is the fluid density,  $\mathbf{u}$  is the velocity vector,  $P$  is the pressure,  $\mathbf{I}$  is the unit diagonal matrix,  $\mathbf{F}$  is the volume force vector,  $\mathbf{H} = \mu(\nabla \mathbf{u} + (\nabla \mathbf{u})^T)$  is the viscous stress tensor, and  $\mu$  is the dynamic viscosity. It was assumed that there are no viscous effects at the slip wall, and hence, the slippage boundary on the solid particles can be expressed by

$$\mathbf{u} \cdot \mathbf{n} = 0 \tag{7}$$

$$\mathbf{H} - (\mathbf{H} \cdot \mathbf{n})\mathbf{n} = 0 \tag{8}$$

where  $\mathbf{n}$  is the normal vector of the flow direction. While the fluid velocity relative to the wall velocity is zero for the no-slip boundary condition on a stationary wall, it can be expressed as  $\mathbf{u} = 0$ .

The creeping flow module in COMSOL Multiphysics was used to solve the gas flow through the 2D Sierpinski carpet models. Methane ( $\text{CH}_4$ ) with density  $\rho = 0.648 \text{ kg/m}^3$ , viscosity  $\mu = 1.1067 \times 10^{-5} \text{ Pa} \cdot \text{s}$ , and mean molecular free path  $\lambda = 6.22 \times 10^{-8} \text{ m}$  was adopted as working gas. The pressure inlet and outlet were settled on the left and right sides of the initial square of the Sierpinski carpet model,

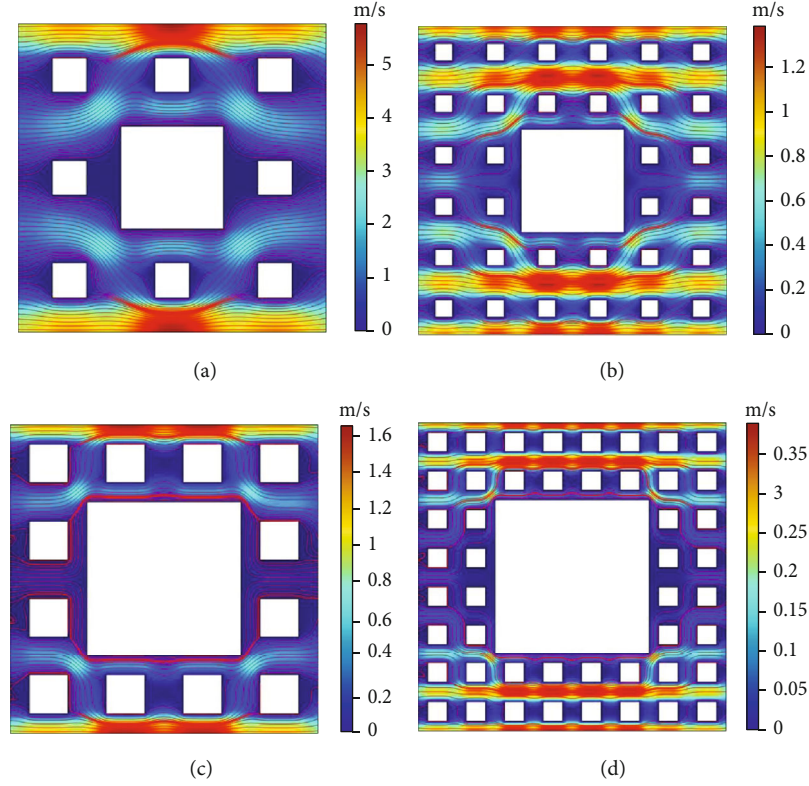


FIGURE 5: The velocity contour with streamlines for the 2nd order of the isotropic Sierpinski carpet models: (a) S1 ( $D_f = 1.893$ ), (b) S5 ( $D_f = 1.934$ ), (c) S2 ( $D_f = 1.792$ ), and (d) S11 ( $D_f = 1.869$ ).

respectively. The pressure difference along the flow direction from left to right was set to be 0.75 Pa. The upper and lower walls of the Sierpinski carpet are symmetrically bordered. The mesh was controlled by a physical mesh in which a free triangle mesh was used. The fluid flow through a porous medium without source terms can be described by Darcy's law.

$$\mathbf{u}_{\text{out}} = -\frac{\mathbf{K}}{\mu} \nabla P, \quad (9)$$

where  $\mathbf{K}$  is the permeability tensor and  $\mathbf{u}_{\text{out}}$  is the flow flux through the porous medium. In most cases, the porous medium is laterally isotropic but vertically anisotropic. If the principal permeability direction is assumed to be along the coordinate axes, the permeability tensor can be expressed as

$$\mathbf{K} = \begin{bmatrix} K_x & 0 \\ 0 & K_y \end{bmatrix}, \quad (10)$$

where  $K_x$  and  $K_y$  are the principal permeabilities along the  $x$  and  $y$  axes, respectively.

### 3. Results and Discussion

In order to validate the present mathematical model, the predicted permeability of the isotropic Sierpinski carpet models

was compared with that of the theoretical models and experimental data. As shown in Figure 3(a), the current fractal model without slippage effect presents acceptable agreement with Kozeny-Carman equation [23] and RTM model [47] as well as available experimental results [48]. It can be seen that the permeability of porous media without slippage effect increases with the increment of porosity. However, the permeability of porous media depends not only on the porosity but also on pore fractal dimension and pore size range [22]. Thus, it is difficult to accurately estimate the permeability of porous media with permeability-porosity relationships such as the Kozeny-Carman equation and its modifications.

Based on the linear correlation for gas permeability of the Klinkenberg equation, the gas slippage factor can be expressed by

$$b_k = \left( \frac{K_g}{K_l} - 1 \right) \bar{P}, \quad (11)$$

where  $K_g$  and  $K_l$  are, respectively, the gas permeability and equivalent liquid permeability (absolute permeability) and  $\bar{P}$  is the mean pressure. Sampath and Keighin [49] proposed Sampath-Keighin (SK) correlation for gas slippage factor based on ten tight sandstone samples as  $b_k = 13.851 (K_l/\phi)^{-0.53}$ . While Florence et al. [50] presented a general square-root (SR) model as  $b_k = \beta (K_l/\phi)^{-0.5}$ , where  $\beta$  is a fitting constant. They obtained an empirical correlation  $\beta = 293.9M^{-0.586}$  with molecular weight ( $M$ ) by fitting the

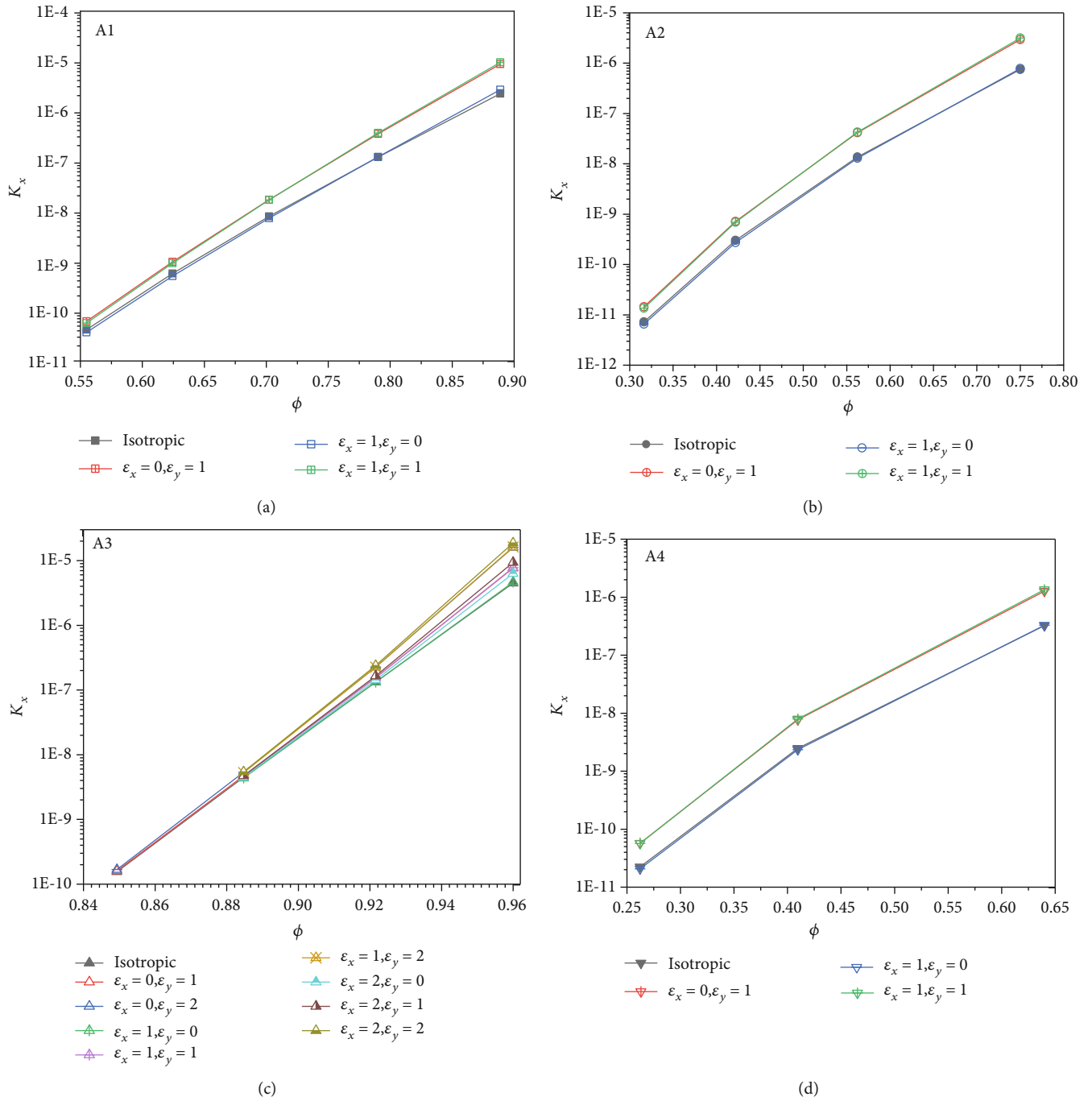


FIGURE 6: Continued.

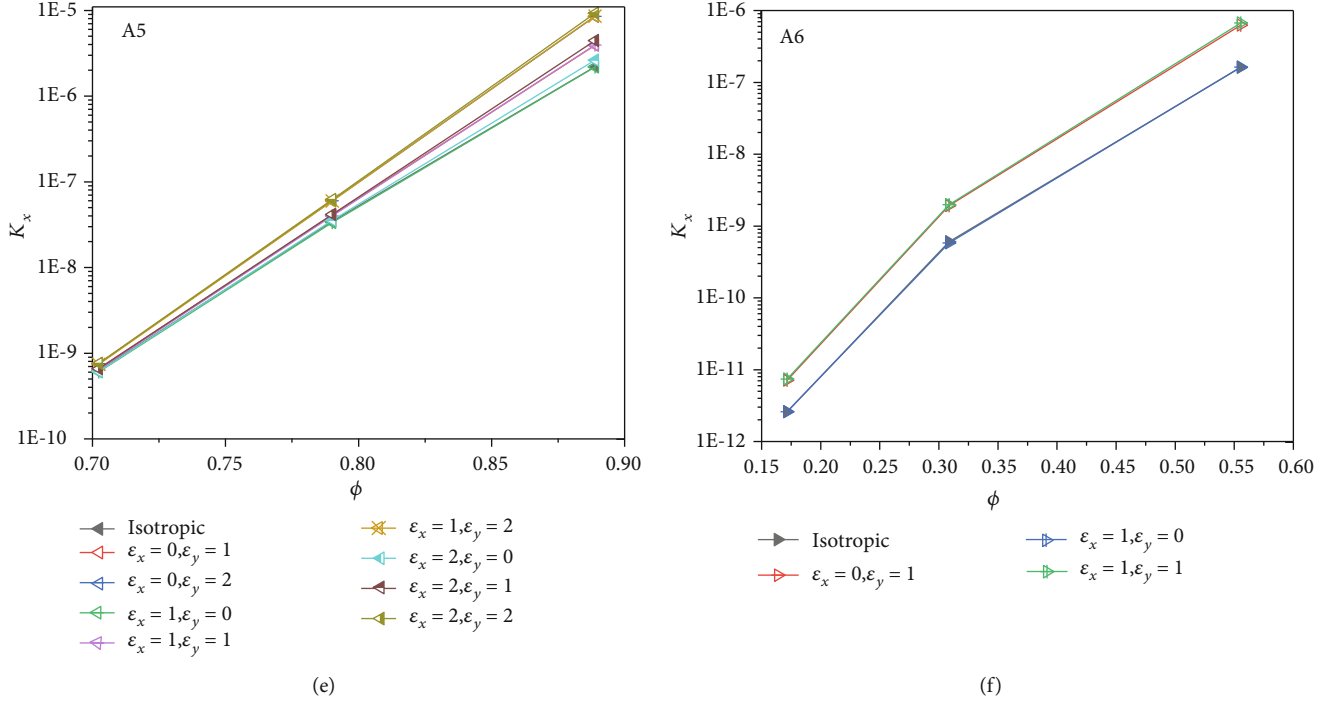


FIGURE 6: The permeability of anisotropic Sierpinski carpet models: (a) A1 ( $D_f = 1.893$ ), (b) A2 ( $D_f = 1.792$ ), (c) A3 ( $D_f = 1.975$ ), (d) A4 ( $D_f = 1.723$ ), (e) A5 ( $D_f = 1.934$ ), and (f) A6 ( $D_f = 1.672$ ).

experimental data for hydrogen, helium, air, nitrogen, and carbon dioxide. As can be seen in Figure 3(b), the calculated gas slippage factors by the present Sierpinski carpet model fall within the predicted range of the SK and SR models.

In order to explore the effect of fractal dimension on the permeability, a pore size range ( $\xi$ ) defined as the ratio of minimum pore size to maximum pore size was introduced. The pore size range of the Sierpinski carpet model can be calculated by  $\xi = n^{1/2}/s^i$ . For example, the pore size range for S1, S2, S5, and S11 are, respectively  $\xi_{S1} = 1/3^i$ ,  $\xi_{S2} = 2/4^i$ ,  $\xi_{S5} = 2/6^i$ , and  $\xi_{S11} = 4/8^i$ . According to Equation (2), the porosity for samples S1 ( $D_f = 1.893$ ) and S5 ( $D_f = 1.934$ ) with same order are the same,  $\phi_{S1} = \phi_{S5} = (8/9)^i$ . While the porosity for samples S2 ( $D_f = 1.792$ ) is same as that of S11 ( $D_f = 1.869$ ) with same order, that is  $\phi_{S2} = \phi_{S11} = (3/4)^i$ . It can be found from Figure 4 that the permeability of the porous media with the same porosity decreases with increased pore fractal dimension. It can be explained as that the proportion of small pores increases as the pore fractal dimension increases under fixed porosity, which induces the increment of tortuosity (Figure 5).

Figure 6 shows the permeability of the anisotropic Sierpinski carpet models (A1-A6). It can be clearly seen from Figure 6 that the permeability of the anisotropic Sierpinski carpet models is different from that of isotropic cases. As shown in Figure 7, the influence of anisotropy induced by  $\epsilon_x \neq 0$  on the gas flow along the  $x$  axis is not evident. Thus, it can be found in Figure 6 that the effect of anisotropy induced by  $\epsilon_x \neq 0$  on the permeability  $K_x$  is marginal. While the anisotropy induced by  $\epsilon_y \neq 0$  can significantly enhance the permeability  $K_x$ , which can be attributed to the large cap-

illaries formed in the case of  $\epsilon_y \neq 0$  (Figures 7(c) and 7(d)). Similar results can be found for the relationship between anisotropy induced by  $\epsilon_x \neq 0$  and the permeability  $K_y$ . Therefore, it can be concluded that the anisotropic factor is beneficial to the vertical fluid flow and can enhance the corresponding permeability.

In order to study the slippage effect in microscale porous media, the slippage boundary was performed on the surface of solid particles in the isotropic Sierpinski carpet models. A dimensionless parameter was defined to characterize the gas slippage effect:

$$\tau = \left| \frac{K_{\text{slip}} - K_{\text{no-slip}}}{K_{\text{no-slip}}} \right|, \quad (12)$$

where  $K_{\text{slip}}$  and  $K_{\text{no-slip}}$  represent the permeability with and without slippage effect, respectively.

Because the pore fractal dimension decreases with the decrease of porosity, it can be found in Figure 8 that the slippage effect strengthens as the pore fractal dimension decreases. However, the slippage effect is not a monotonically decreasing function with porosity for certain groups of samples with the same pore fractal dimension ( $D_f = 1.862$ ,  $D_f = 1.896$ ,  $D_f = 1.934$ ,  $D_f = 1.969$ ,  $D_f = 1.975$ , and  $D_f = 1.989$ ). The reduced pore size by decreasing porosity can enhance slippage effect. While the increased proportion of solid particles by decreasing porosity can increase flow resistance and then lower the slippage effect. Therefore, the slippage parameter  $\tau$  may decrease when the porosity decrease for the samples with a certain pore fractal dimension because the increased flow resistance takes a dominate effect on gas

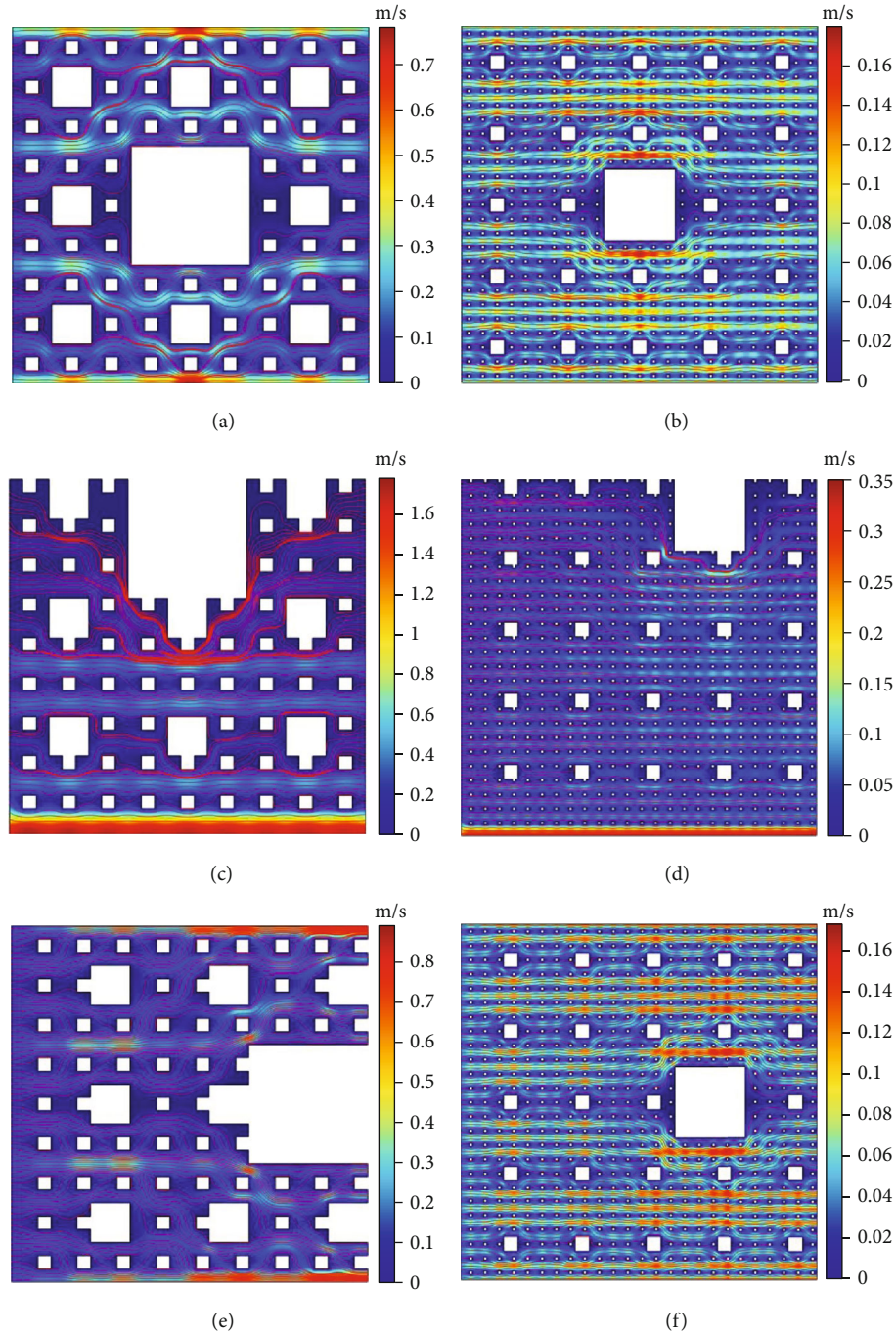


FIGURE 7: The velocity contour with streamlines for the 3rd order of anisotropic Sierpinski carpet models: (a) A1 (isotropic), (b) A3 (isotropic), (c) A1 ( $\epsilon_x = 0, \epsilon_y = 1$ ), (d) A3 ( $\epsilon_x = 1, \epsilon_y = 2$ ), (e) A1 ( $\epsilon_x = 1, \epsilon_y = 0$ ), and (f) A3 ( $\epsilon_x = 1, \epsilon_y = 0$ ).

slippage. It should be noted that only gas slippage effect in the micro- and nanoscale pores has been taken into account in the present work, other microscale effect such as transition flow and free molecular flow may be included when the Knudsen number is larger than 0.1.

#### 4. Conclusions

In this work, a two-dimensional Sierpinski carpet model has been adopted to characterize the multiscale microstructures

of porous media. And a pore-scale mathematical model has been developed to study the gas flow through both the isotropic and anisotropic porous media. The influence of microstructures and anisotropy as well as slippage effect on the permeability has been discussed. It has been found that the permeability of porous media depends on the porosity and pore fractal dimension as well as pore size range. The value of permeability increases with increased porosity and decreases as pore fractal dimension increases under fixed porosity. The flow field and permeability of anisotropic

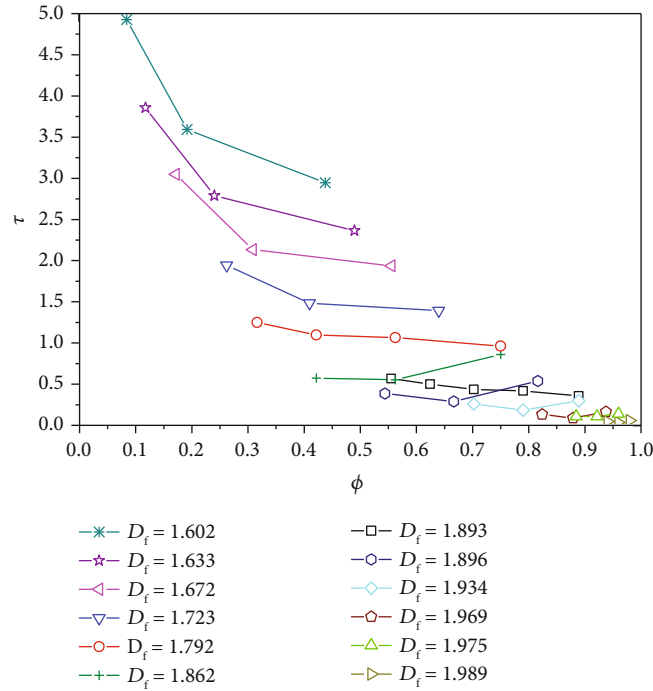


FIGURE 8: The effect of slippage effect on the permeability of the Sierpinski carpet models.

porous media are different from that of isotropic porous media. The anisotropic factor is beneficial to the vertical fluid flow and can enhance the corresponding permeability. For the microscale porous media, gas slippage phenomena show a significant effect on the effective permeability. The numerical results indicate that the slippage effect strengthens as the pore fractal dimension decreases. However, it may be reduced by increased porosity under certain pore fractal dimensions as two competitive factors (pore size and flow resistance) are involved. The proposed fractal model shows advantages in characterizing the complex and irregular microstructures of porous media and provides a conceptual tool to understand the flow mechanisms of gas flow through the porous media. It should be pointed out that some complications such as dead-end pores, contact and overlap of solid particles, pore/particle configurations, and morphology were neglected in the proposed fractal model. As an extension to this study, it would be helpful to investigate randomly a three-dimensional fractal model.

### Data Availability

The numerical data used to support the findings of this study are available from the corresponding author upon request.

### Conflicts of Interest

The authors declare that there is no conflict of interest regarding the publication of this paper.

### Acknowledgments

This work was jointly supported by the Natural Science Foundation of China (grant numbers 51876196, 51736007, and 21873087), the Zhejiang Provincial Natural Science Foundation of China (grant number LR19E060001), and the State Key Laboratory Cultivation Base for Gas Geology and Gas Control of Henan Polytechnic University (grant number WS2018A02).

### References

- [1] M. Sahimi, *Flow and Transport in Porous Media and Fractured Rock: From Classical Methods to Modern Approaches*, Wiley-VCH, Weinheim, 2011.
- [2] K. Vafai, *Handbook of Porous Media*, CRC Press, Boca Raton, FL, USA, 2019.
- [3] P. Xu, A. P. Sasmito, and A. S. Mujumdar, *Heat and Mass Transfer in Drying of Porous Media*, CRC Press, Boca Raton, FL, USA, 2019.
- [4] E. Charlaix, A. P. Kushnick, and J. P. Stokes, "Experimental study of dynamic permeability in porous media," *Physical Review Letters*, vol. 61, no. 14, pp. 1595–1598, 1988.
- [5] P. M. Adler and J. F. Thovert, "Real porous media: local geometry and macroscopic properties," *Applied Mechanics Reviews*, vol. 51, no. 9, pp. 537–585, 1998.
- [6] X. Cui, A. M. M. Bustin, and R. M. Bustin, "Measurements of gas permeability and diffusivity of tight reservoir rocks: different approaches and their applications," *Geofluids*, vol. 9, no. 3, pp. 208–223, 2009.
- [7] Z. Yang, Z. Ma, Y. Luo, Y. Zhang, H. Guo, and W. Lin, "A measured method for in situ viscosity of fluid in porous media by

- nuclear magnetic resonance,” *Geofluids*, vol. 2018, Article ID 9542152, 8 pages, 2018.
- [8] A. Koponen, M. Kataja, and J. Timonen, “Permeability and effective porosity of porous media,” *Physical Review E*, vol. 56, no. 3, pp. 3319–3325, 1997.
- [9] L. Hao and P. Cheng, “Lattice Boltzmann simulations of anisotropic permeabilities in carbon paper gas diffusion layers,” *Journal of Power Sources*, vol. 186, no. 1, pp. 104–114, 2009.
- [10] P. Xu, B. Yu, X. Qiao, S. Qiu, and Z. Jiang, “Radial permeability of fractured porous media by Monte Carlo simulations,” *International Journal of Heat and Mass Transfer*, vol. 57, no. 1, pp. 369–374, 2013.
- [11] R. Guibert, P. Horgue, G. Debenest, and M. Quintard, “A comparison of various methods for the numerical evaluation of porous media permeability tensors from pore-scale geometry,” *Mathematical Geosciences*, vol. 48, no. 3, pp. 329–347, 2016.
- [12] X. Yan, Z. Huang, J. Yao et al., “Numerical simulation of hydro-mechanical coupling in fractured vuggy porous media using the equivalent continuum model and embedded discrete fracture model,” *Advances in Water Resources*, vol. 126, pp. 137–154, 2019.
- [13] R. Liu, N. Huang, Y. Jiang, H. Jing, and L. Yu, “A numerical study of shear-induced evolutions of geometric and hydraulic properties of self-affine rough-walled rock fractures,” *International Journal of Rock Mechanics and Mining Sciences*, vol. 127, article 104211, 2020.
- [14] M. J. Blunt, *Multiphase Flow in Permeable Media: A Pore-Scale Perspective*, Cambridge University Press, Cambridge, 2017.
- [15] B. B. Mandelbrot, *The Fractal Geometry of Nature*, Freeman, New York, NY, USA, 1982.
- [16] A. J. Katz and A. H. Thompson, “Fractal sandstone pores: implications for conductivity and pore formation,” *Physical Review Letters*, vol. 54, no. 12, pp. 1325–1328, 1985.
- [17] E. Perfect and B. D. Kay, “Applications of fractals in soil and tillage research: a review,” *Soil & Tillage Research*, vol. 36, no. 1–2, pp. 1–20, 1995.
- [18] B. Yu, “Analysis of flow in fractal porous media,” *Applied Mechanics Reviews*, vol. 61, no. 5, article 050801, 2008.
- [19] B. Wang, Y. Jin, Q. Chen, J. Zheng, Y. Zhu, and X. Zhang, “Derivation of permeability-pore relationship for fractal porous reservoirs using series-parallel flow resistance model and lattice Boltzmann method,” *Fractals*, vol. 22, no. 3, article 1440005, 2014.
- [20] P. Xu, “A discussion on fractal models for transport physics of porous media,” *Fractals*, vol. 23, no. 3, article 1530001, 2015.
- [21] Y. Jin, X. Liu, H. Song, J. Zheng, and J. Pan, “General fractal topography: an open mathematical framework to characterize and model mono-scale-invariances,” *Nonlinear Dynamics*, vol. 96, no. 4, pp. 2413–2436, 2019.
- [22] B. Yu and P. Cheng, “A fractal permeability model for bi-dispersed porous media,” *International Journal of Heat and Mass Transfer*, vol. 45, no. 14, pp. 2983–2993, 2002.
- [23] P. Xu and B. Yu, “Developing a new form of permeability and Kozeny–Carman constant for homogeneous porous media by means of fractal geometry,” *Advances in Water Resources*, vol. 31, no. 1, pp. 74–81, 2008.
- [24] W. Wei, J. Cai, J. Xiao, Q. Meng, B. Xiao, and Q. Han, “Kozeny–Carman constant of porous media: insights from fractal-capillary imbibition theory,” *Fuel*, vol. 234, pp. 1373–1379, 2018.
- [25] B. Yu, J. Li, Z. Li, and M. Zou, “Permeabilities of unsaturated fractal porous media,” *International Journal of Multiphase Flow*, vol. 29, no. 10, pp. 1625–1642, 2003.
- [26] P. Xu, S. Qiu, B. Yu, and Z. Jiang, “Prediction of relative permeability in unsaturated porous media with a fractal approach,” *International Journal of Heat and Mass Transfer*, vol. 64, pp. 829–837, 2013.
- [27] P. Xu, C. Li, S. Qiu, and A. P. Sasmito, “A fractal network model for fractured porous media,” *Fractals*, vol. 24, no. 2, article 1650018, 2016.
- [28] J. Cai, D. Lin, H. Singh, W. Wei, and S. Zhou, “Shale gas transport model in 3D fractal porous media with variable pore sizes,” *Marine and Petroleum Geology*, vol. 98, pp. 437–447, 2018.
- [29] Y. Xia, J. Cai, E. Perfect, W. Wei, Q. Zhang, and Q. Meng, “Fractal dimension, lacunarity and succolarity analyses on CT images of reservoir rocks for permeability prediction,” *Journal of Hydrology*, vol. 579, article 124198, 2019.
- [30] S. W. Coleman and J. C. Vassilicos, “Transport properties of saturated and unsaturated porous fractal materials,” *Physical Review Letters*, vol. 100, no. 3, article 035504, 2008.
- [31] Y. Chen, C. Shen, P. Lu, and Y. Huang, “Role of pore structure on liquid flow behaviors in porous media characterized by fractal geometry,” *Chemical Engineering and Processing*, vol. 87, pp. 75–80, 2015.
- [32] A. E. Khabbazi, J. Hinebaugh, and A. Bazylak, “Analytical tortuosity–porosity correlations for Sierpinski carpet fractal geometries,” *Chaos, Solitons and Fractals*, vol. 78, pp. 124–133, 2015.
- [33] H. Rostamzadeh, M. R. Salimi, and M. Taeibi-Rahni, “Permeability correlation with porosity and Knudsen number for rarefied gas flow in Sierpinski carpets,” *Journal of Natural Gas Science and Engineering*, vol. 56, pp. 549–567, 2018.
- [34] Y. Kuwata and K. Suga, “Direct numerical simulation of turbulence over anisotropic porous media,” *Journal of Fluid Mechanics*, vol. 831, pp. 41–71, 2017.
- [35] J. Cao, H. Gao, L. Dou, M. Zhang, and T. Li, “Modeling flow in anisotropic porous medium with full permeability tensor,” *Journal of Physics: Conference Series*, vol. 1324, no. 1, article 012054, 2019.
- [36] F. Javadpour, D. Fisher, and M. Unsworth, “Nanoscale gas flow in shale gas sediments,” *Journal of Canadian Petroleum Technology*, vol. 46, no. 10, pp. 55–61, 2007.
- [37] L. M. Pant, S. K. Mitra, and M. Secanell, “Absolute permeability and Knudsen diffusivity measurements in PEMFC gas diffusion layers and micro porous layers,” *Journal of Power Sources*, vol. 206, pp. 153–160, 2012.
- [38] H. Wang, W. Xu, J. Shao, and F. Skoczylas, “The gas permeability properties of low-permeability rock in the process of triaxial compression test,” *Materials Letters*, vol. 116, pp. 386–388, 2014.
- [39] K. Wu, Z. Chen, and X. Li, “Real gas transport through nanopores of varying cross-section type and shape in shale gas reservoirs,” *Chemical Engineering Journal*, vol. 281, pp. 813–825, 2015.
- [40] C. Li, P. Xu, S. Qiu, and Y. Zhou, “The gas effective permeability of porous media with Klinkenberg effect,” *Journal of Natural Gas Science and Engineering*, vol. 34, pp. 534–540, 2016.
- [41] L. Wu, M. T. Ho, L. Germanou et al., “On the apparent permeability of porous media in rarefied gas flows,” *Journal of Fluid Mechanics*, vol. 822, pp. 398–417, 2017.

- [42] J. Wang, L. Yu, and Q. Yuan, "Experimental study on permeability in tight porous media considering gas adsorption and slippage effect," *Fuel*, vol. 253, pp. 561–570, 2019.
- [43] X. Li, Z. Gao, S. Fang, C. Ren, K. Yang, and F. Wang, "Fractal characterization of nanopore structure in shale, tight sandstone and mudstone from the Ordos basin of China using nitrogen adsorption," *Energies*, vol. 12, no. 4, p. 583, 2019.
- [44] Y. Ichikawa and A. P. S. Selvadurai, *Transport Phenomena in Porous Media: Aspects of Micro/Macro Behaviour*, Springer, Heidelberg, 2012.
- [45] K. S. Lee and T. H. Kim, *Integrative Understanding of Shale Gas Reservoirs*, Springer, Switzerland, 2016.
- [46] Y. Feng, B. Yu, M. Zou, and D. Zhang, "A generalized model for the effective thermal conductivity of porous media based on self-similarity," *Journal of Physics D: Applied Physics*, vol. 37, no. 21, pp. 3030–3040, 2004.
- [47] R. Gauvin, A. Kerachni, and B. Fisa, "Variation of mat surface density and its effect on permeability evaluation for RTM modelling," *Journal of Reinforced Plastics and Composites*, vol. 13, no. 4, pp. 371–383, 2016.
- [48] S. N. Ehrenberg and P. H. Nadeau, "Sandstone vs. carbonate petroleum reservoirs: a global perspective on porosity-depth and porosity-permeability relationships," *AAPG Bulletin*, vol. 89, no. 4, pp. 435–445, 2005.
- [49] K. Sampath and C. W. Keighin, "Factors affecting gas slippage in tight sandstones," *SPE/DOE Low Permeability Symposium*, *SPE*, vol. 9872, pp. 27–29, 1981.
- [50] F. A. Florence, J. Rushing, K. E. Newsham, and T. A. Blasingame, "Improved permeability prediction relations for low permeability sands," in *Rocky Mountain Oil & Gas Technology Symposium*, Denver, Colorado, U.S.A, April 2007.